Supporting Information for: Assembly of Polyelectrolyte Star Block Copolymers at the Oil-Water Interface

Jan-Michael Y. Carrillo,*,† Zhan Chen,‡ Uvinduni I. Premadasa,¶ Christian Steinmetz,‡ E. Bryan Coughlin,‡ Benjamin Doughty,*,¶ Thomas P. Russell,*,‡,§ and Bobby G. Sumpter†

†*Center for Nanophase Materials Sciences, Oak Ridge National Laboratory, Oak Ridge, Tennessee 37831, United States*

‡*Polymer Science and Engineering Department, Conte Center for Polymer Research, University of Massachusetts, Amherst, MA 01003, United States*

¶*Chemical Sciences Division, Oak Ridge National Laboratory, Oak Ridge, Tennessee 37831, United States*

§*Materials Sciences Division, Lawrence Berkeley National Laboratory, Berkeley, CA 94720, United States*

E-mail: carrillojy@ornl.gov; doughtybl@ornl.gov; russell@mail.pse.umass.edu

Contents

1 Simulations Details

We performed coarse-grained molecular dynamics simulations to probe the effect of star diblock copolymers on the interfacial energy of the dielectric solvent/oil interface. We represented the star block copolymer as connected coarse-grained beads with neutral polystyrene segments (PS) and positively charged quaternized poly(2-vinylpyridine) (P2VP) segments with explicit negatively charged counterions. The model consisted mainly of three components, which are the star diblcok copolymers, the dielectric solvent phase, and the oil phase. In this coarse-grained representation, all short-range pair-wise interactions are described by a shifted truncated Lennerd-Jones (LJ, Eq.S1) potential with a characteristic bead size σ, cutoff r_c, and strength of interaction ε_{LJ}.

$$U_{LJ}(r_{ij}) = \begin{cases} 4\varepsilon_{LJ}\left[\left(\frac{\sigma}{r_{ij}}\right)^{12} - \left(\frac{\sigma}{r_{ij}}\right)^{6} - \left(\frac{\sigma}{r_{cut}}\right)^{12} + \left(\frac{\sigma}{r_{cut}}\right)^{6}\right] & r_{ij} \leq r_{cut} \\ 0 & r_{ij} > r_{cut} \end{cases} \tag{S1}$$

All bond connectivity is described by finite extensible non-linear elastic (FENE, Eq.S2) bonds[1] with spring constant $k_{bond} = 30k_BT/\sigma^2$, maximum bond extent $R_o = 1.5\sigma$, thermal energy k_BT, and the second term is cutoff at $2^{1/6}\sigma$.

$$U_{FENE}(r) = \frac{1}{2}k_{bond}R_o^2 \ln\left[1 - \left(\frac{r}{R_o}\right)^2\right] + 4k_BT\left[\left(\frac{\sigma_f}{r}\right)^{12} - \left(\frac{\sigma_f}{r}\right)^{6}\right] + k_BT \tag{S2}$$

The degree-of-polymerization of the arm of the star block copolymer is L_{arm} and there are N_{arm} arms in a star molecule. In an arm, the number of PS and P2VP beads are equal (or the mole fraction of PS in an arm is $f = 0.5$).

The next component in the model is the dielectric solvent which is represented as charged dumbbells having 2 opposite charges with a magnitude of q and separated by a distance of $\sim 0.5\sigma$ via a FENE bond with $\sigma_f = 0.475\sigma$. The pairwise interactions of dielectric solvent beads include both short-range LJ interactions and long-range Coulomb interaction (Eq.S3) with Bjerrum length $l_B = 1\sigma$ through the particle–particle particle–mesh (PPPM) method.[2]

$$U_{Coul}(r_{ij}) = k_B T \frac{l_B q_i q_j}{r_{ij}} \tag{S3}$$

The static dielectric constant of the solvent is estimated through the variance of the system dipole moment[3,4] in an isothermal-isobaric (NPT) ensemble simulation of a simulation box containing only solvents as,

$$\epsilon = 1 + \frac{1}{3V k_B T \epsilon_o} \left(\left\langle \vec{M}^2 \right\rangle - \left\langle \vec{M} \right\rangle^2 \right) \tag{S4}$$

where $\vec{M}$ is the system dipole moment, $\vec{M} = \Sigma_i \vec{\mu}_i$ where $\mu_i = q_i \vec{r}_i$ is the dipole of particle i. The value of the static dielectric constant, ϵ, can be tuned by changing the value of q as seen in Fig. S1. Finally, the oil phase is represented as LJ beads where the oil and solvent is incompatible, PS is miscible to oil and P2VP is slightly less miscible to oil beads relative to PS beads. The pair-wise non-bonded potential parameters are summarized in Tab. S1. The simulation consisted of either 5000 or 20000 solvent molecules (10000 or 40000 solvent beads), 5000 or 20000 oil beads, $N_{arm} = \{1, 2, 3, 4\}$ and number of stars, $m_{star} = \{3 - 180\}$ or a bulk star density, $\phi_s = N_{arm} m_{star} / N_{oil} = 0.024 - 0.36\ \sigma^{-3}$.

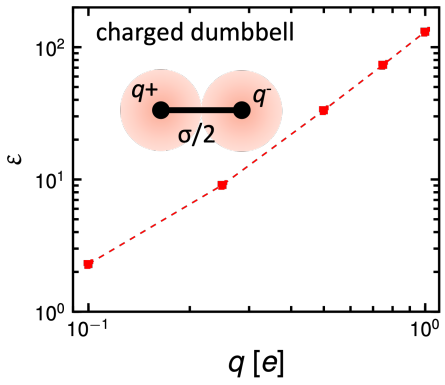

Figure S1: Dependence of the static dielectric constant, ϵ, of a simulation box composed of 3×10^4 charged dumbbells with charge q^+ and q^-.

The simulation consisted of several steps, which included an initial equilibration isothermal-isobaric ensemble (NPT) step, NPT equilibration where protonation is incorporated as described in the *ad hoc* reaction in Fig. 1Simulation box showing a single star or multiple stars

Table S1: Lennard-Jones (LJ) interaction parameters and bead charge q.

Pair	ε_{LJ} $[k_BT]$	r_c $[\sigma]$	q $[e]$
solven-solvent	1.0	2.5	± 0.25
solvent-PS	0.3	2.5	–
solvent-P2VP	0.5	2.5	–
solvent-counterion	1.0	2.5	–
solvent-oil	0.3	2.5	–
solvent-QP2VP	1.0	2.5	–
solvent-IP2VP	0.5	2.5	–
PS-PS	1.0	2.5	0
PS-P2VP	0.3	2.5	–
PS-counterion	1.0	$2^{1/6}$	–
PS-oil	1.0	2.5	–
PS-QP2VP	0.3	2.5	–
PS-IP2VP	0.3	2.5	–
P2VP-P2VP	1.0	2.5	0
P2VP-counterion	1.0	$2^{1/6}$	–
P2VP-oil	0.9	2.5	–
P2VP-QP2VP	1.0	2.5	–
P2VP-IP2VP	1.0	2.5	–
counterion-counterion	1.0	$2^{1/6}$	-1
counterion -oil	1.0	$2^{1/6}$	–
counterion -QP2VP	1.0	$2^{1/6}$	–
counterion -IP2VP	1.0	$2^{1/6}$	–
oil-oil	1.0	2.5	0
oil-QP2VP	0.9	2.5	–
oil-IP2VP	0.9	2.5	–
QP2VP-QP2VP	1.0	2.5	$+1$
QP2VP-IP2VP	1.0	2.5	–
IP2VP-IP2VP	1.0	2.5	0

at the dielectric solvent-oil interface (a). Cyan beads are lyophilic beads representing PS, blue beads are quaternized P2VP or QP2VP, green beads are inert P2VP beads or IP2VP, pink rods are dielectric solvent molecules representing the aqueous phase and oil beads are not shown for clarity. Atomistic and coarse-grained representation of a 3-arm PS-P2VP block copolymer star (b). *Ad hoc* protonation reaction where a dipolar solvent molecule is consumed when the positively charged end of the solvent molecule comes into contact with a P2VP bead (within a 1.3 σ cutoff). The P2VP bead is quarternized to QP2VP, which is positively charged, and a counterion is dissociated (c).figure.caption.1(c), NPT equilibration where the reaction is turned off, and by a canonical (NVT) production run. The temperature is maintained by coupling the system to a Langevin thermostat,[5] such that the motion of the beads can be described as,

$$m_i \frac{d\vec{v}_i(t)}{dt} = \vec{F}_i(t) - \xi \vec{v}_i(t) + \vec{F}_i^R(t) \tag{S5}$$

where $m_i = 1$ is the bead mass, $\vec{v}_i(t)$ is the bead velocity, and $\vec{F}_i(t)$ denotes the net deterministic force acting on the i^{th} bead. The stochastic force $\vec{F}_i^R(t)$ has a zero average value $\left\langle \vec{F}_i^R(t) \right\rangle = 0$ and δ-functional correlations $\left\langle \vec{F}_i^R(t) \cdot F_i^R(t') \right\rangle = 6k_BT\xi\delta(t-t')$. The bead friction coefficient ξ is set to $\xi = 1/7.0\ m/\tau$ where τ is the reduced time unit $\tau = \sigma(m/k_BT)^{1/2}$. A Berendsen barostat[6] is used to control pressure in the equilibration stage where the damping parameter was set to 5.0 τ. The deformation of the simulation box to adjust the system pressure was coupled in the x, y directions but not in the z direction with setpoint $P = 0\ k_BT/\sigma^3$ in the lateral (x and y) direction and $P = 0.08\ k_BT/\sigma^3$ in the normal (z) direction.

Following the initial equilibration NPT run, the NPT run with the *ad hoc* reaction was carried out until all P2VP were converted to QP2VP. The *ad hoc* reaction was implemented using the package developed by Gissenger et al.[7,8] We monitored the reaction kinetics of the protonation of P2VP to QP2VP by following the depletion of [P2VP]/[P2VP]$_0$ relative to its original concentration and found that the reaction is first-order. (see Fig. S2) This step was

followed by another NPT equilibration run to equilibrate the system after the protonation reaction.

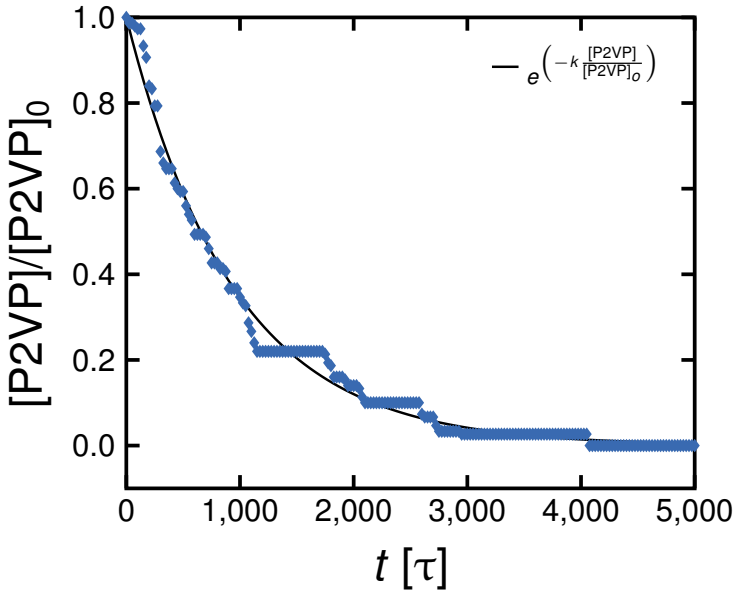

Figure S2: Protonation reaction kinetics of a simulation box with $m_{star} = 10$, $f_q = 1.0$ and $\phi_s = 0.06$. The black line is a fit to first-order reaction kinetics.

In the production NVT runs, the simulation box was deformed to the average dimensions determined in the NPT runs. The NPT equilibration runs (including the protonation reaction step) proceeded for up to 3.0×10^4 τ and the NVT production run proceeded for up to 1.0×10^4 τ. The velocity-Verlet algorithm with a time step of $\Delta t = 0.005$ τ was used for integrating the equations of motion in Eq.S5. All simulations were performed using the LAMMPS molecular dynamics simulations software package.[9,10]

2 Experiment Details

2.1 ^{1}H-NMR

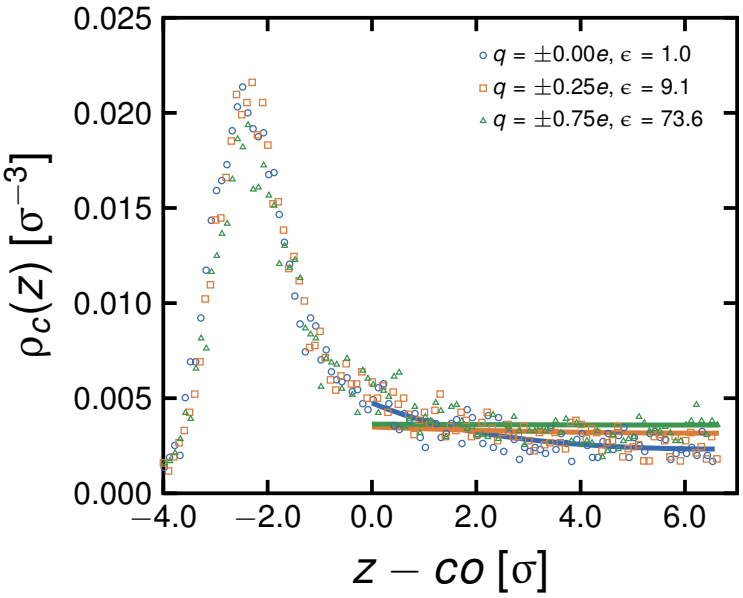

Figure S3: Counterion density distribution, $\rho_c(z)$, for the systems with $N_{arm} = 3$, $m_{star} = 10$, $\phi_s = 0.06$ $f_q = 0.4$ and in oil-solvent interface at solvents with different dielectric constant, ϵ. Lines are fits to Eq.5. Note that fits for $\rho_c(z)$ near $z = co$ is best for the lowest value of ϵ suggesting a gradient of ϵ near the diffuse counterion-star interface that is in between the ϵ of oil ($\epsilon = 1$) and the solvent.

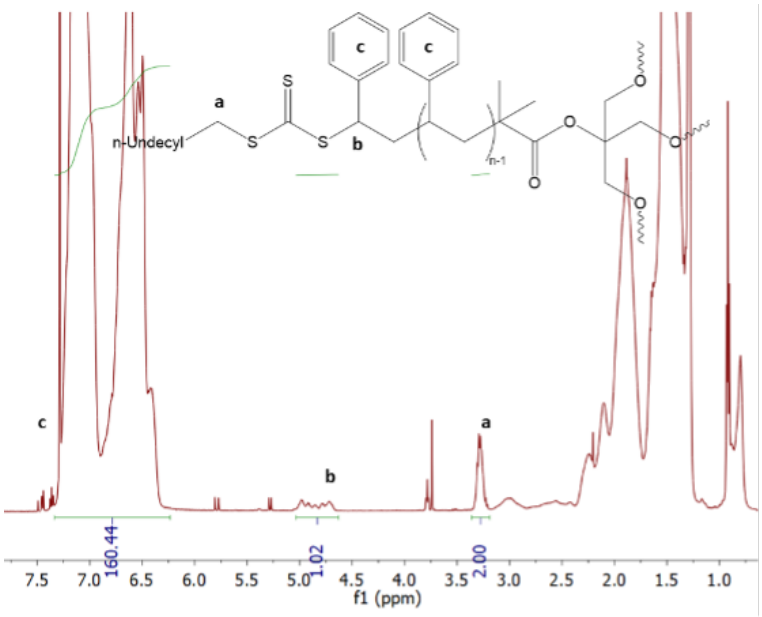

Figure S4: ^{1}H-NMR of sample 4-arm polystyrene core in deuterated chloroform.

2.2 GPC

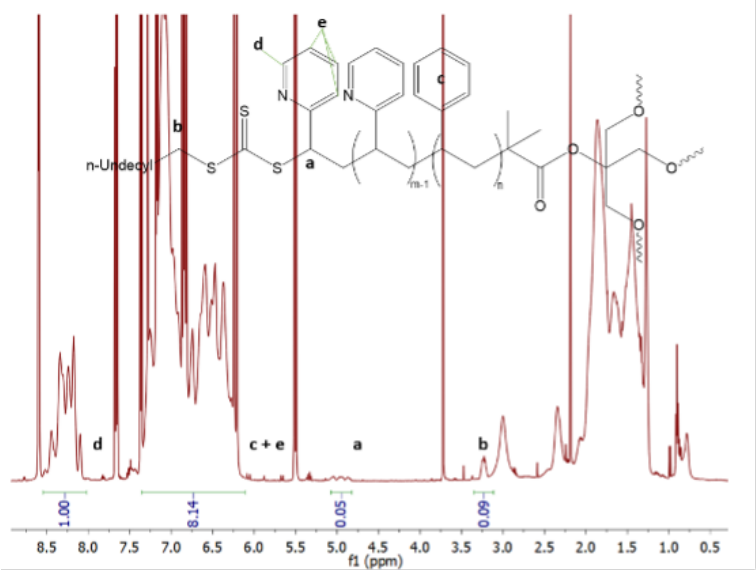

Figure S5: ^{1}H-NMR of sample 4-arm star block copolymers after growing 2VP from 4-arm PS core block precursor in deuterated chloroform.

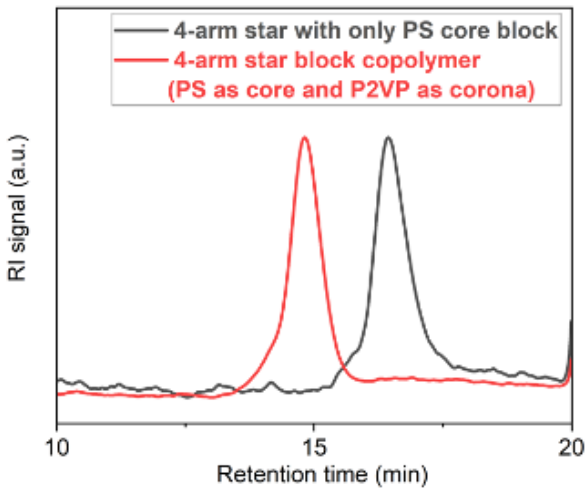

Figure S6: GPC traces of 4-arm star block copolymers in DMF.

References

(1) Kremer, K.; Grest, G. S. Dynamics of Entangled Linear Polymer Melts: A Molecular-Dynamics Simulation. *J. Chem. Phys.* **1990**, *92*, 5057–5086.

(2) Hockney, R. W.; Eastwood, J. W. *Computer Simulation Using Particles*; crc Press,

2021.

(3) Raabe, G.; Sadus, R. J. Molecular Dynamics Simulation of the Dielectric Constant of Water: The Effect of Bond Flexibility. *J. Chem. Phys.* **2011**, *134*, 234501.

(4) Neumann, M. Dipole Moment Fluctuation Formulas in Computer Simulations of Polar Systems. *Mol. Phys.* **1983**, *50*, 841–858.

(5) Schneider, T.; Stoll, E. Molecular-Dynamics Study of a Three-Dimensional One-Component Model for Distortive Phase Transitions. *Phys. Rev. B* **1978**, *17*, 1302.

(6) Berendsen, H. J.; Postma, J. v.; van Gunsteren, W. F.; DiNola, A.; Haak, J. R. Molecular Dynamics with Coupling to an External Bath. *J. Chem. Phys.* **1984**, *81*, 3684–3690.

(7) Gissinger, J. R.; Jensen, B. D.; Wise, K. E. Modeling Chemical Reactions in Classical Molecular Dynamics Simulations. *Polymer* **2017**, *128*, 211–217.

(8) Gissinger, J. R.; Jensen, B. D.; Wise, K. E. Reacter: A Heuristic Method for Reactive Molecular Dynamics. *Macromolecules* **2020**, *53*, 9953–9961.

(9) Plimpton, S. Fast Parallel Algorithms for Short-Range Molecular Dynamics. *J. Comput. Phys.* **1995**, *117*, 1–19.

(10) Brown, W. M.; Wang, P.; Plimpton, S. J.; Tharrington, A. N. Implementing Molecular Dynamics on Hybrid High Performance Computers–Short Range Forces. *Comput. Phys. Commun.* **2011**, *182*, 898–911.